Sci. Technol. Adv. Mater. **12** (2011) 055008 (10pp) doi:10.1088/1468-6996/12/5/055008

β-TCP porous pellets as an orthopaedic drug delivery system: ibuprofen/carrier physicochemical interactions

Hiba Baradari, Chantal Damia, Maggy Dutreih-Colas, Eric Champion, Dominique Chulia and Marylène Viana

SPCTS—Centre Européen de la Céramique, 12 Rue Atlantis, 87068 Limoges CEDEX, France

E-mail: hiva.baradari@etu.unilim.fr

Received 4 July 2011
Accepted for publication 10 August 2011
Published 29 September 2011
Online at stacks.iop.org/STAM/12/055008

Abstract
Calcium phosphate bone substitute materials can be loaded with active substances for *in situ*, targeted drug administration. In this study, porous β-TCP pellets were investigated as an anti-inflammatory drug carrier. Porous β-TCP pellets were impregnated with an ethanolic solution of ibuprofen. The effects of contact time and concentration of ibuprofen solution on drug adsorption were studied. The ibuprofen adsorption equilibrium time was found to be one hour. The adsorption isotherms fitted to the Freundlich model, suggesting that the interaction between ibuprofen and β-TCP is weak. The physicochemical characterizations of loaded pellets confirmed that the reversible physisorption of ibuprofen on β-TCP pellets is due to Van der Waals forces, and this property was associated with the 100% ibuprofen release.

Keywords: beta tricalcium phosphate, porous pellets, drug delivery system, drug adsorption, ibuprofen

1. Introduction

Calcium phosphate (CaP) bioceramics have a chemical composition similar to that of human bone. This property makes them a biocompatible material that is widely used as a bone substitute for orthopaedic applications [1]. Aside from biocompatibility, integration of a porous network in a CaP implant facilitates bone ingrowth and vascularization. Porous osteoconductive bioceramics thus have been developed to mimic the porous architecture of trabecular bone. Hence, the advantage of a porous structure, containing macropores (pore size >80–$100\,\mu$m) and micropores (pore size $<10\,\mu$m), is providing appropriate spaces for bone ingrowth and improving body fluid flow through the bone graft [2].

Post-operative pathologies, like infection or inflammation of bone sites, can affect bone healing processes. Therefore, incorporating drug substances such as anti-inflammatories and antibiotics, which could be gradually released *in situ*, is of great interest in the development of orthopaedic drug delivery systems (DDSs). Porous bioceramic matrices are good candidates for hosting drug molecules, as drug substances can be loaded inside the pores of the drug carrier and released *in situ* [3]. Thus, the combination of CaP porous bioceramics with therapeutic agents meets the requirements of an ideal bone substitute by providing biocompatibility, osteoconductivity and effective drug administration to reduce implantation side effects.

Different types of CaP ceramics, such as hydroxyapatite (HA) [4], beta-tricalcium phosphate (β-TCP) [5], biphasic calcium phosphate (BCP) [6], amorphous calcium phosphate (ACP) [7] and calcium-deficient HA (CDHA) [8], have been studied as drug carriers in orthopaedic DDS applications. Among the different compositions of CaP materials, beta-tricalcium phosphate (β-TCP–$Ca_3(PO_4)_2$) has attracted attention owing to its bioresorbability, which permits a gradual replacement of the implant by the newly formed bone [1, 9]. The drug delivery ability of β-TCP has been investigated in numerous studies in combination with, for example, bone morphogenetic proteins [10], cefuroxime [11], vancomycin [12], gentamicin [13] and sulbactam [14]. In the mentioned examples [10–14], the feasibility of β-TCP as a potential drug carrier has been proved, its drug release

behaviour *in vitro* and/or *in vivo* has been shown and the effect of parameters such as carrier porosity or chemical composition of β-TCP on drug delivery has been discussed. However, the type of interaction between the drug and the β-TCP drug carrier, which is an important factor in controlling drug release kinetics, has been highlighted in only a few studies [5, 15].

Ibuprofen is one of the most widely used nonsteroidal analgesic and anti-inflammatory model drugs because of its short biological half-life (2 h) and good pharmacological activity. Besides, its molecule size of about 0.6–1.0 nm allows its free propagation through the pore channels of host porous materials [16, 17]. As mentioned above, adding an antiinflammatory drug in such systems can attenuate the local inflammatory response to the implantation process. Such drug delivery system can also be used for the local treatment of articular inflammatory pathologies such as arthritis. In previous studies [18–22], porous β-TCP pellets were produced by high-shear wet granulation and loaded with ibuprofen by solvent evaporation method. The spherical form and the size of these implants, 900 μm in diameter, can guarantee the filling of complex-shaped bone cavities, while maintaining intergranular spaces of about 180 μm for bone ingrowth. Besides, such spherical porous granules are interesting for drug delivery applications because of their controlled surface, which allows the deposition of regular and reproducible amounts of therapeutic agents [22].

In this study, we investigated the interaction between ibuprofen and β-TCP pellets to determine the characteristics of this DDS and explain the drug release behaviour as a function of drug/carrier interactions. β-TCP porous pellets were fabricated by wet high shear granulation as in previous works [18–22]. The obtained pellets were loaded through impregnation: they were soaked in ibuprofen solutions, separated from their supernatant and then dried under ambient conditions. The adsorption kinetics of ibuprofen and adsorption capacity of the porous pellets were determined by varying the contact time and the concentration of ibuprofen solutions. The ibuprofen adsorption reversibility was investigated via ibuprofen desorption isotherms. The type of interactions between ibuprofen and β-TCP pellets was studied by x-ray diffraction, Fourier transform infrared (FTIR) spectroscopy and Raman scattering. The ibuprofen release profile was then obtained in a phosphate buffered solution at 37 °C.

2. Materials and methods

2.1. Preparation of porous β-TCP pellets

Porous β-TCP pellets were fabricated by wet high-shear granulation followed by spheronization in a Mi-Pro high-shear granulator (Pro-C-epT, Zelzate, Belgium) as described in previous works [18,19]. Tricalcium phosphate powder ($Ca_3(PO_4)_2$, Cooper, France) and pregelatinized starch (Sepistab ST 200, Seppic, France) were used as granule skeleton and binder/pore former, respectively. Granules were dried in a fluidized bed dryer (Glatt, Haltingen Binzen/Baden, Germany) for 20 min at 60 °C and sieved to retain the 710–1000 μm fraction. The pellets were then annealed at 270 °C for 2 h to remove the pore former and calcined at 900 °C for 15 min in a furnace (Vecstar Ltd, UK) to obtain β-TCP phased pellets [23] with improved mechanical properties.

2.2. Drug loading

Ibuprofen 50 (BASF, Germany) was used as the therapeutic agent. The adsorption experiments were performed in triplicate by soaking 350 mg of porous pellets in ethanolic solutions of ibuprofen (technical ethanol, 96 wt%), under ambient conditions and without agitation. After a given contact time, loaded granules were separated from their supernatant and dried overnight under ambient conditions. Ibuprofen loading was performed in two different regimes:

(1) soaking the pellets in 4 ml of a 100 mg ml^{-1} ibuprofen solution for a period ranging between 10 min and 14 days (adsorption kinetics), and
(2) soaking the pellets in 4 ml of solution and ibuprofen concentrations from 50 to 300 mg ml^{-1} for 1 h (adsorption isotherms).

On the basis of the high solubility limit of ibuprofen in ethanol, 428 mg ml^{-1} at 20 °C [24], the adsorbed amount of ibuprofen was directly quantified by immersing loaded samples in 40 ml of ethanol for 4 h. The eluted ibuprofen concentration was measured by UV absorption spectrophotometry (Lambda 20, Elmer Perkin, USA) at $\lambda =$ 264 nm. The adsorbed amount (Q) of ibuprofen was deduced as

$$Q(\text{mmol m}^{-2}) = \times \frac{\text{Adsorbed ibuprofen quantity (mmol)}}{\text{Sample mass(g)} \times \text{specific surface area (m}^2\,\text{g}^{-1})}, \quad (1)$$

and the drug content (DC%) was calculated as

$$\text{DC\%} = \left[\frac{\text{Adsorbed ibuprofen mass (mg)}}{\text{Loaded sample mass (mg)}}\right] \times 100. \quad (2)$$

Ibuprofen desorption isotherms were obtained from pellets loaded with the impregnation solution containing 300 mg ml^{-1} ibuprofen. After 1 h of contact, the impregnation medium was diluted with ethanol to lower the ibuprofen concentrations to 150, 100 and 50 mg ml^{-1}. The pellets were then kept in contact with these solutions for 1 h. After that, they were separated from the supernatants, and the adsorbed amount of ibuprofen was measured following the same procedure as described for the adsorption experiments.

2.3. Physicochemical characterizations

β-TCP porous pellets were characterized before and after treatment with an ibuprofen solution of 200 mg ml^{-1} for 1 h to (1) document the properties of β-TCP porous pellets and (2) investigate ibuprofen/β-TCP interactions. We also studied

the physicochemical characteristics of β-TCP pellets after ibuprofen desorption in 40 ml of ethanol for 4 h.

X-ray powder diffraction (XRD) patterns were collected using CuKα radiation ($\lambda = 1.5406$ Å) and a $\theta/2\theta$ diffractometer (D8, Bruker) with a step size of 0.02° and a count time of 2 s. Phases were identified by comparing the diffraction patterns with the International Center for Diffraction Data (ICDD) Powder Diffraction Files (00-09-0432 for HA, 00-09-0169 for β-TCP and 00-034-1728 for ibuprofen) using EVA software (Bruker AXS).

FTIR measurements (Spectrum One, Perkin-Elmer) were performed on samples prepared by mixing granules (1 wt%) with KBr powder. The spectra were collected in the range of 4000–400 cm^{-1} at ambient temperature, with a resolution of 2 cm^{-1}. Raman spectra were recorded in the 250–3700 cm^{-1} range, using a Jobin Yvon spectrometer and an argon-ion laser (514.5 nm, Stabilite 2017 Spectra physics). Samples were observed using a field emission gun scanning electron microscope (FEG-SEM, Jeol JSM-7400 F) without coating them.

The pycnometric density (d_{pycno}, g cm^{-3}) was determined using a helium pycnometer AccuPyc 1330 (Micromeritics Instruments Inc, Norcross, GA, USA). Prior to the measurements, the samples were degassed for 3 days at 30 °C in a vacuum better than 50 mTorr (VacPrep 061, Micromeritics Instruments Inc). The measurements were repeated until the density stabilized [25].

Specific surface area (SSA, $m^2\,g^{-1}$) was measured by nitrogen adsorption using a Gemini 2360 Analyser (Micromeritics Instruments Inc.) and calculated according to the Brunauer–Emmet–Teller equation [26]. Prior to the measurements, the samples were degassed under the same conditions as for pycnometric density determination.

Porosity measurements were carried out using a mercury intrusion porosimeter (Autopore IV 9500; Micromeritics Instruments Inc) equipped with a 5 cm^3 powder penetrometer. Cumulative and incremental mercury intrusion volumes were evaluated. The intrusion volume (V_{intra}, ml g^{-1}), which corresponds to the open porosity of the pellet, was deduced and associated with the corresponding pore size diameters. The total porosity (%) was calculated as

$$\text{Total porosity}(\%) = \frac{V_{intra}}{V_{solid} + V_{intra}} \times 100, \qquad (3)$$

where V_{solid} is the solid volume, determined from the pycnometric density.

2.4. In vitro ibuprofen release

Dissolution tests [18] were performed on pellets loaded for 1 h with a solution containing 200 g l^{-1} ibuprofen. Unloaded pellets were also tested and used as reference. The measurements were carried out in triplicate until obtaining the constant released amount, using a phosphate buffered solution (pH = 7.5) at 37 °C as the dissolution medium. The released amount of ibuprofen was determined at regular intervals by UV absorption spectrophotometry at 264 nm. The flow-through cell apparatus described in European Pharmacopea [27] was used for this purpose. It was equipped with tablet cells of 12 mm thickness. A ruby bead of 5 mm diameter and glass beads of 1 mm diameter were placed at the apex of the flow-through cell to ensure laminar flow of the 100 ml of dissolution medium, entering into the cell at a flow rate of 2 ml min^{-1}. Accurately weighed loaded granules (275 mg) were placed on the glass bead bed. The automated system CE 7smart (Sotax, Basel, Switzerland) was linked to a piston pump CP7–35 (Sotax, Basel, Switzerland) and a UV–VIS spectrophotometer (Lambda 20, Elmer Perkin, USA) for a direct online analysis of the filtered sample.

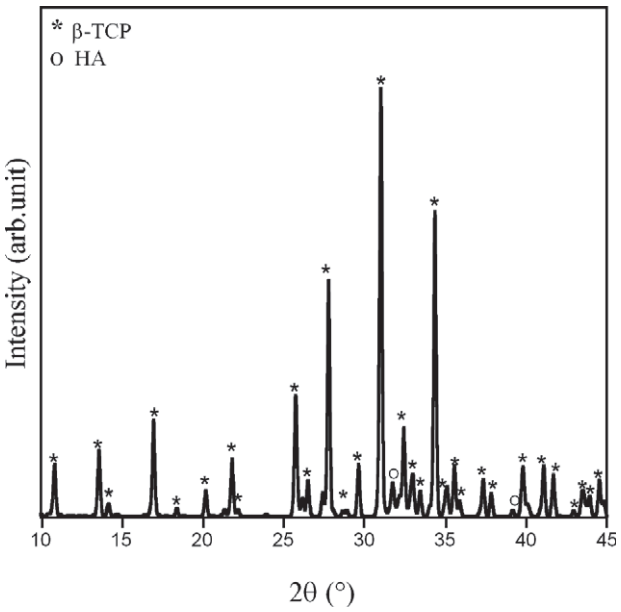

Figure 1. XRD pattern of β-TCP pellets.

The dissolution profile, i.e. cumulative percentage of released ibuprofen (q, %) versus time (t, h), was then plotted. To determine the release mechanism, the results were fitted with the Higuchi and Hixson–Crowell models, which characterize diffusion and erosion contributions, respectively. The Higuchi equation is [28]:

$$q(\%) = \text{at}^{1/2} + \text{b}, \qquad (4)$$

where a is the release rate (%/$h^{1/2}$) and b is a constant; the Hixson–Crowell model is [29]:

$$\sqrt[3]{100} - \sqrt[3]{100 - q} = \text{ct} + \text{d}, \qquad (5)$$

where c is the release rate.

3. Results

3.1. β-TCP pellets characteristics

The XRD pattern of the granules after heat treatment at 900 °C shows that they are mainly composed of well-crystallized β-TCP with a minute HA fraction (figure 1). The proportions of HA and β-TCP phases and the Ca/P molar ratio were calculated using integrated intensities of characteristic diffraction peaks of the granules calcined at 1000 °C for 15 h

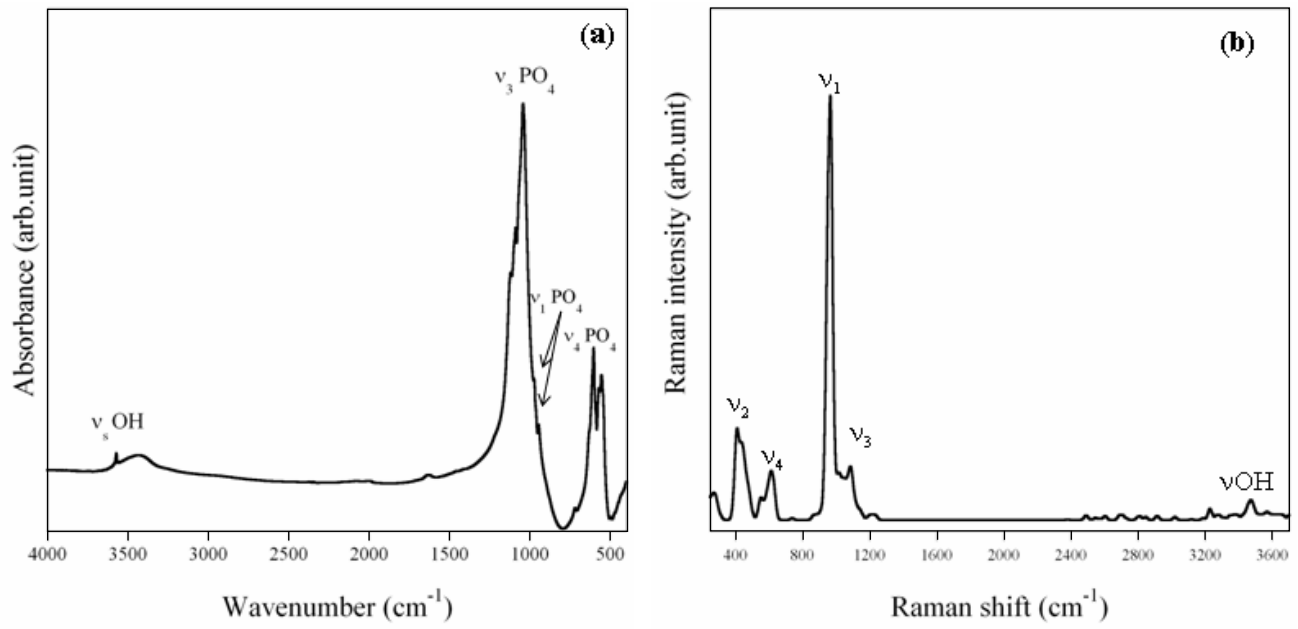

Figure 2. (a) FTIR and (b) Raman spectra of β-TCP porous pellets.

(data not shown) [30]. The Ca/P molar ratio was 1.512 and the final product consisted of more than 92 wt% β-TCP. The presence of HA stemmed from the composition of the initial commercial powder, which was used for pellet preparation: 80 wt% monetite and 20 wt% HA; the heat treatment at 900 °C resulted in their transformation into the stable β-TCP phase with residual HA [23].

The typical bands of β-TCP can be observed in the FTIR absorption spectra of the pellets (figure 2(a)). The bands at 570 and 630 cm^{-1} are attributed to the bending vibration mode (ν_4) of the O–P–O group. The 969 and 947 cm^{-1} peaks are due to the ν_1 symmetric stretching of the P–O bond, and the signals at 1100 and 1040 cm^{-1} are assigned to the triply degenerate antisymmetric stretching mode (ν_3) of the P–O bond [31]. Additionally, the absorption bands assigned to the O-H group (3546 cm^{-1}) indicate that a small amount of HA phase was present in the final products, confirming the XRD results. The absorption bands of H_2O around 3400 cm^{-1} indicate the H_2O adsorption on the pellet surface.

The Raman spectrum of β-TCP porous pellets is shown in figure 2(b). The peaks related to the doubly degenerate ν_2 and triply degenerate ν_4 bending modes of the PO_4 group (O–P–O moiety) span the frequency ranges of 370–500 and 530–645 cm^{-1}, respectively. The symmetric stretching mode (ν_1) of the tetrahedral PO_4 group (P–O bond) is detected at 962 cm^{-1}. Peaks observed in the range of 1030–1100 cm^{-1} originate from the degenerated asymmetric stretching mode (ν_3) of the PO_4 group (P–O bond). Similar to the FTIR spectrum, the weak signal at 3573 cm^{-1} associated with the stretching O–H^- mode reveals the presence of a minor HA phase [32, 33] in the β-TCP pellets.

The obtained pellets have a surface area of $5.48 \pm 0.04\ m^2\ g^{-1}$, a pycnometric density of $3.04 \pm 0.01\ g\ cm^{-3}$ and a total open porosity of 58% (0.45 ml g^{-1}). The pore size distribution (figure 3) is bimodal, with small pores of 80–300 nm (80% of the total pore volume) and larger 300–2000 nm pores (20% of the total pore volume).

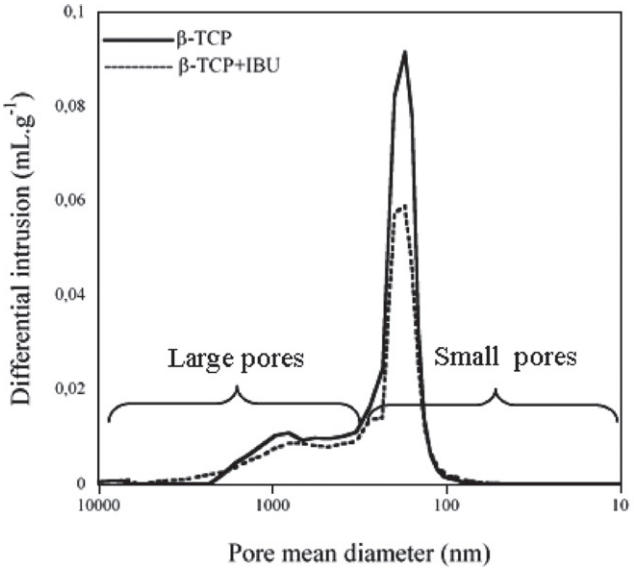

Figure 3. Pore size distribution in β-TCP and ibuprofen-loaded β-TCP pellets (β-TCP + IBU).

The presence of these two pore types is confirmed from the surface morphology observations of the pellets (figure 4). The formation of large pores results from starch elimination, whereas small ones are due to the incomplete densification of initial grains after the calcination at 900 °C. The surface morphology of the pellets (figure 4(c)) shows individual grains smaller than 1 μm. They are partially sintered after heat treatment at 900 °C for 15 min. The smooth edges and necks between particles are produced by the thermal treatment.

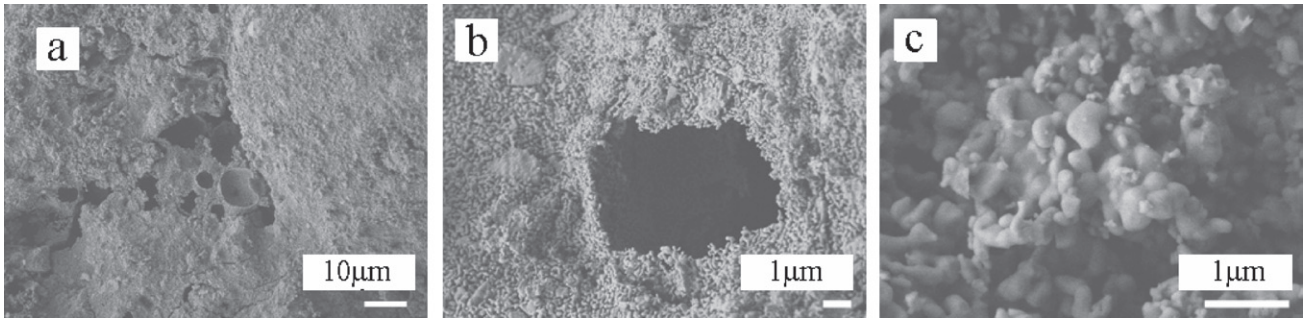

Figure 4. SEM images of β-TCP pellets.

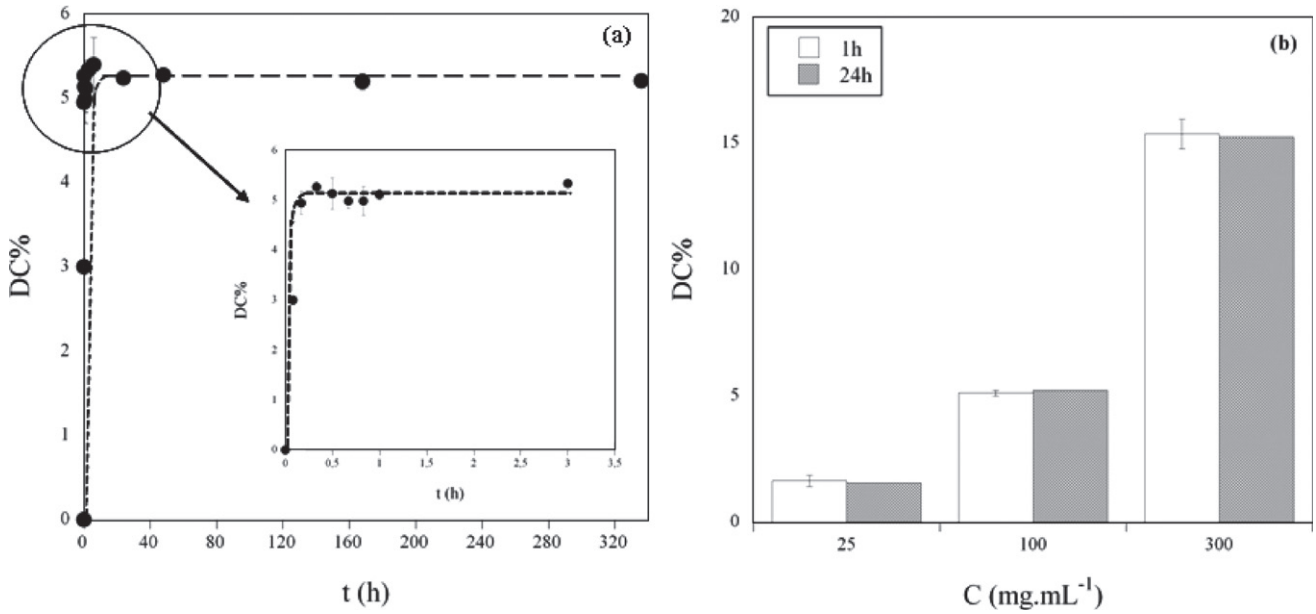

Figure 5. (a) Adsorption kinetics (C = 100 g l^{-1}) and (b) DC% as a function of ibuprofen solution concentration and immersion time ($t_1 = 1$ h, $t_2 = 24$ h).

3.2. Drug adsorption behaviour

The drug adsorption was studied by varying two parameters: immersion time to establish ibuprofen adsorption kinetics and the ibuprofen solution concentration to obtain the drug adsorption isotherm.

Figure 5(a) shows the adsorption kinetics of ibuprofen ($C = 100$ g l^{-1}). The drug loading is a nonlinear function of immersion time: a fast uptake is observed during the first hour and the DC% remains constant at 5.18 ± 0.14% for up to two weeks. To confirm the equilibrium time of one hour, the β-TCP pellets were loaded with solutions having two different drug concentrations (25 and 300 g l^{-1}), for 1 and 24 h. As shown in figure 5(b), increasing the ibuprofen concentration raises the DC%, but extending the immersion time from 1 to 24 h does not affect the DC%. Thus, 1 h was adopted as the equilibrium time in the following experiments.

The adsorption and desorption isotherms are indicated in figure 6 by open and solid symbols, respectively. The adsorption isotherm correlates linearly with DC% and the drug concentration in solution. DC% increases from

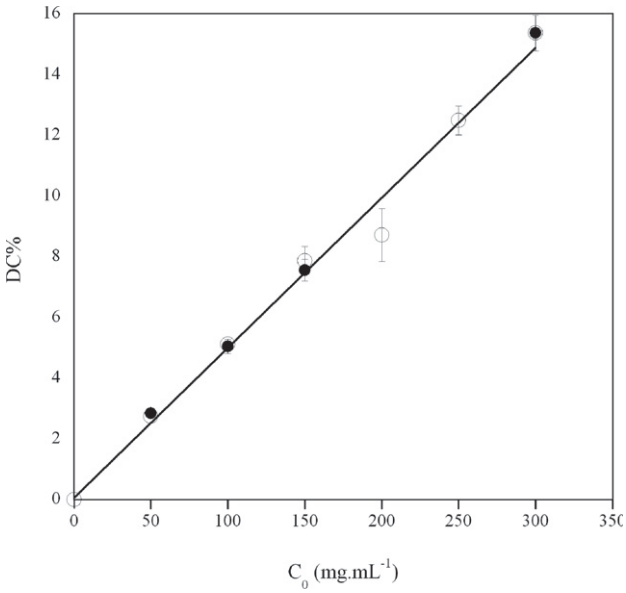

Figure 6. (o) Adsorption and (•) desorption isotherms ($t = 1$ h).

Table 1. Ibuprofen adsorption data.

C (g l^{-1})	C (mol l^{-1})	Q (mmol m^{-2}) (mean ± SD)	C_e^a (mol l^{-1})	DC% (mean ± SD)
50	0.24	0.03 ± 0.01	0.23 ± 0.01	2.75 ± 0.06
100	0.48	0.05 ± 0.01	0.46 ± 0.01	5.1 ± 0.1
150	0.73	0.08 ± 0.01	0.69 ± 0.01	7.9 ± 0.5
200	0.96	0.10 ± 0.01	0.92 ± 0.01	8.3 ± 0.9
250	1.21	0.13 ± 0.01	1.15 ± 0.01	12.5 ± 0.5
300	1.45	0.16 ± 0.01	1.38 ± 0.01	15.4 ± 0.6

[a] $C_e = C$-(Q × SSA/4).

(2.75 ± 0.06)% to (15.37 ± 0.58)% over the entire ibuprofen concentration range without reaching a plateau (figure 6). The adsorption isotherm fits to the Freundlich equation $Q = aC_e^m$, where Q is the adsorbed drug amount (mmol m^{-2}), C_e is the equilibrium concentration (mol l^{-1}), and a (ml m^{-2}) and m are constants reflecting the adsorption affinity and capacity, respectively [34]. The C_e and Q pairs are listed in table 1. The constants a and m were deduced as 0.11 ml m^{-2} and 1, respectively, by linearizing the isotherm equation ($\ln Q = \ln a + m \ln C_e$). The good fit of the ibuprofen adsorption data ($R^2 = 0.9816$) with the Freundlich adsorption model indicates a weak affinity between the adsorbent and adsorbate [35], here, β-TCP and ibuprofen, respectively.

The obtained desorption isotherm is superimposed with the adsorption isotherm. It follows the same linear trend ($R^2 = 0.9991$), indicating that the ibuprofen adsorption on the β-TCP pellets is reversible.

3.3. Loaded β-TCP pellet characterisation

Pellets loaded with the 200 mg ml^{-1} ibuprofen solution were further characterized to locate ibuprofen on the pellets and to determine the type of interactions between the drug and the carrier. These pellets contained 0.10 ± 0.01 mmol m^{-2} (Q) ibuprofen corresponding to a DC% of 8.27 ± 0.87% (table 1).

Figures 7(a) and 7(b) show SEM images of ibuprofen and loaded pellets, respectively. A comparison between the initial (rod-like crystals) and adsorbed ibuprofen reveals that the morphology of ibuprofen is modified during adsorption on the pellets. Very fine ibuprofen filaments are present between asperities of the pellet surface.

Figure 8 shows the XRD patterns of the β-TCP pellets before and after drug loading, revealing that the β-TCP pellets maintain their crystalline structure after the loading. Characteristic diffraction peaks of the initial crystalline ibuprofen are visible in the XRD pattern of the loaded pellets, indicating that the adsorbed ibuprofen has a crystalline structure.

Figure 9(a) shows the FTIR spectra of ibuprofen and β-TCP loaded with ibuprofen. The typical PO_4^{3-} bands of βTCP are found in the latter spectrum. The C–H$_x$ peaks around 3000–2850 cm^{-1} and the band assigned to the C = O stretching mode of the –COOH group at 1720 cm^{-1} confirm the adsorption of ibuprofen onto the β-TCP pellets. The absorption bands assigned to the quaternary carbon atom (1462 and 1520 cm^{-1}), tertiary carbon atom (1340 cm^{-1}) and O–H bending vibration (1421 cm^{-1}) of ibuprofen [36] overlap with the PO_4^{3-} bands and are invisible in the spectrum of the loaded β-TCP. Therefore, Raman measurements were performed to characterize the adsorbed ibuprofen. The advantage of this technique over FTIR absorption is that the $\nu_1(PO_4)$ mode of β-TCP appears as an intense peak, and the other stretching modes of the PO_4 group (i.e. ν_2, ν_3 and ν_4) have low Raman intensities (figure 2(b)) and do not overlap with the ibuprofen peaks. Besides, Raman peaks are more pronounced than FTIR peaks in ibuprofen.

Indeed, the characteristic peaks of ibuprofen are visible in the Raman spectrum of the loaded pellets (figure 9(b)). As in pure ibuprofen, this spectrum contains the stretching bands of C–H$_x$ (ν C–H$_x$) between 3100 and 2700 cm^{-1}, consisting of symmetric and asymmetric stretching vibrations of = C–H and –C–H groups. The position of the asymmetric C = C (ν C = C) stretch at 1608 cm^{-1} is also similar to that of the Raman spectrum of pure ibuprofen. CO–H (H-bonded) bending modes of ibuprofen (i.e. δ(CO-H)) at 1432, 1227, 1124, 662 and 637 cm^{-1} are also present in the spectrum of the loaded pellets [37].

The physical characteristics of the pellets before and after ibuprofen loading are summarized in table 2. The drug adsorption causes a slight decrease in the specific surface area of the pellets from 5.49 ± 0.05 to 4.85 ± 0.05 m^2 g^{-1} and a reduction of the total porosity from 57 to 50%. As illustrated in figure 3, the decrease in pore volume is stronger for small pores (29%) than for large pores (20%). This pore filling is caused by the penetration of the drug solution inside the porous network and the deposition, after solvent evaporation, of the amount of drug corresponding to the concentration of the liquid inside the pores. The quantity of ibuprofen adsorbed in the pore volume of 0.45 ml g^{-1} from the 200 mg ml^{-1} ibuprofen solution is 90 mg g^{-1}. This is less than the amount measured by UV spectrophotometry (106 mg g^{-1}) because some ibuprofen is present on the outer surface of the pellets, as illustrated in figure 7.

3.4. β-TCP pellet characterization after ibuprofen desorption

Figures 10(a) and 10(b) show the XRD pattern and FTIR spectrum of the β-TCP pellets after ibuprofen desorption in ethanol, respectively. They reveal a lack of structural modification of β-TCP upon ibuprofen loading (cf figures 1 and 2, respectively). Residual ibuprofen could not be detected by any characterization method used in this study.

3.5. In vitro ibuprofen release

Figure 11 shows the dissolution profile, i.e. cumulative percentage of ibuprofen released versus time, revealing fast release from the β-TCP porous pellets. The lag time of about 3 min is the time required to obtain a homogenous drug distribution in the release medium. The profile consists of two phases: a fast release of about 70% of adsorbed ibuprofen within 15 min followed by a slow release of the remaining 30%. The total release takes 60 min. These results confirm the complete ibuprofen release from the β-TCP porous pellets. Moreover, no modification of the pellets has been observed at the end of the dissolution trial.

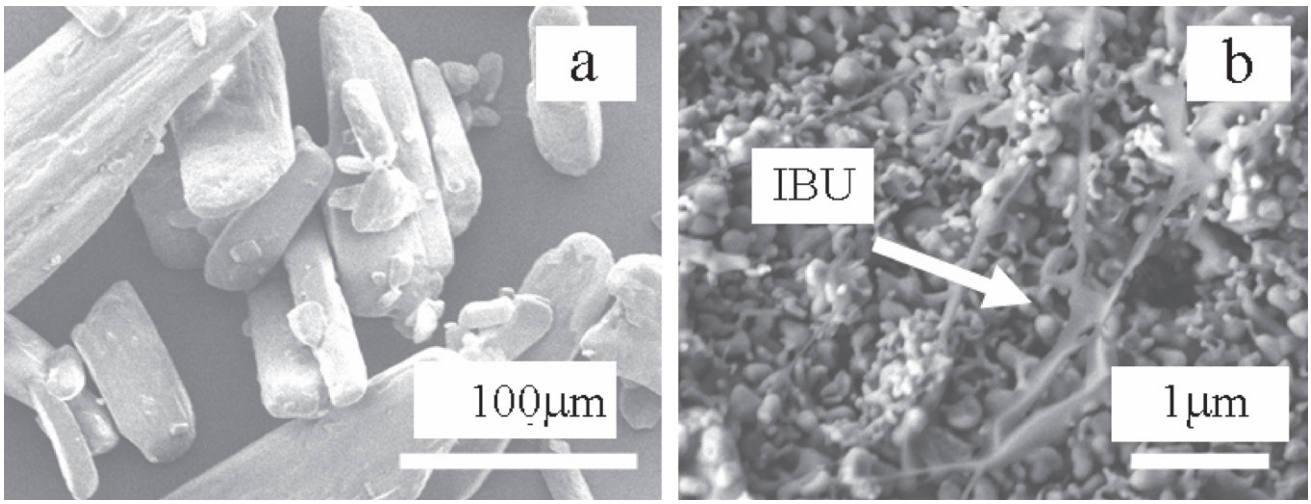

Figure 7. SEM images of (a) ibuprofen and (b) β-TCP pellets loaded with ibuprofen (β-TCP + IBU).

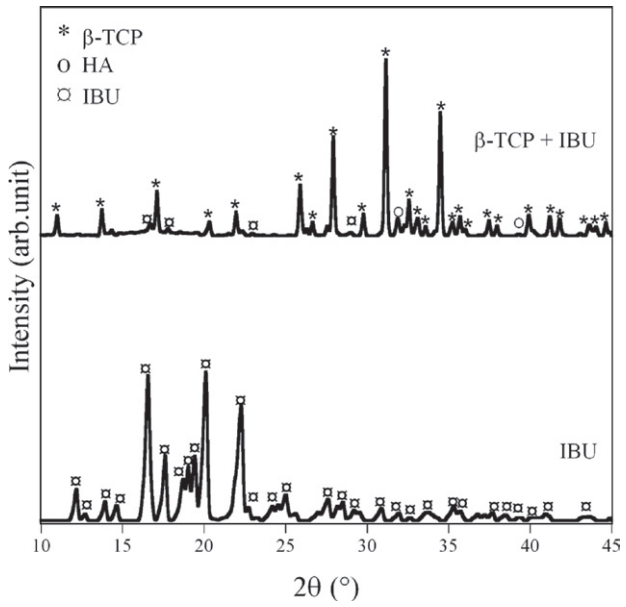

Figure 8. XRD patterns of ibuprofen (IBU) and β-TCP pellets loaded with ibuprofen (β-TCP + IBU).

The dissolution data were fitted by the Higuchi and HixonCrowell equations to determine the release mechanism. The fitting was performed separately for the first and second release phases. Comparison of the correlation coefficients (R^2, table 3) indicates that both phases fit better to the Hixson–Crowell model, implying that the release of ibuprofen is controlled by drug erosion from internal and external surfaces of the β-TCP pellets.

4. Discussion

The previous works concerning β-TCP/ibuprofen delivery systems for bone substitution applications [19, 20] demonstrated the feasibility of producing porous pellets by high-shear wet granulation, followed by heat treatment. The drug loading by vacuum impregnation and solvent evaporation allowed the complete deposition of the anti-inflammatory agent present in the loading solution. The objective of this work was to investigate the ibuprofen adsorption mechanisms. Therefore, the drug loading was performed by immersing β-TCP pellets in the drug solution and removing the supernatant after various immersion times.

We found that ibuprofen uptake by the β-TCP pellets reaches equilibrium within one hour. Charney *et al* [38] have shown that ibuprofen molecules diffuse with the solvent into the pores by capillarity and remain trapped there after solvent removal. The adsorption equilibrium time for the β-TCP pellets can be defined as the time needed by the pores to be saturated by a given liquid, here ibuprofen solution. As shown in a study by Stähli *et al* [35], the impregnation of a porous object, dipped in a liquid, occurs when the liquid can penetrate the porous network through capillary rise while air exits from the scaffold. Therefore, capillary rise proceeds as long as air can move out of the capillary under the capillary pressure. It has been shown that β-TCP porous pellets sized between 710 and 1000 μm contain an open-pore network with a total open porosity of 57%. Thus, the adsorption equilibrium time could be related to the time required to reach equilibrium between the capillary pressure and the pressure of air trapped inside capillaries.

The adsorbed amount of ibuprofen increases linearly with the drug concentration in the adsorption solution, without saturation. The same linear behaviour was observed by Gburek *et al* [35] for the adsorption of vancomycin on brushite, monetite and hydroxyapatite. The obtained adsorption isotherms fit to a Freundlich-type equation, indicating weak adsorption [34]. The physicochemical characterizations of ibuprofen-loaded pellets confirm the weak affinity between the adsorbate and adsorbent.

The lack of changes in the Raman signals of PO_4^{3-} groups indicates that the β-TCP structure was not affected by the ibuprofen adsorption. The same conclusion can be drawn for ibuprofen, indicating that the ibuprofen adsorption on the β-TCP porous pellets proceeds via physisorption.

Table 2. Physical characteristics of pellets before and after drug loading.

Sample	SSA ($m^2\ g^{-1}$)	Total porosity(%)	Total pore volume ($ml\ g^{-1}$)	Small pore volume ($ml\ g^{-1}$)	Large pore volume ($ml\ g^{-1}$)
β-TCP	5.48	57	0.45	0.35	0.10
β-TCP + IBU	4.85	50	0.33	0.25	0.08

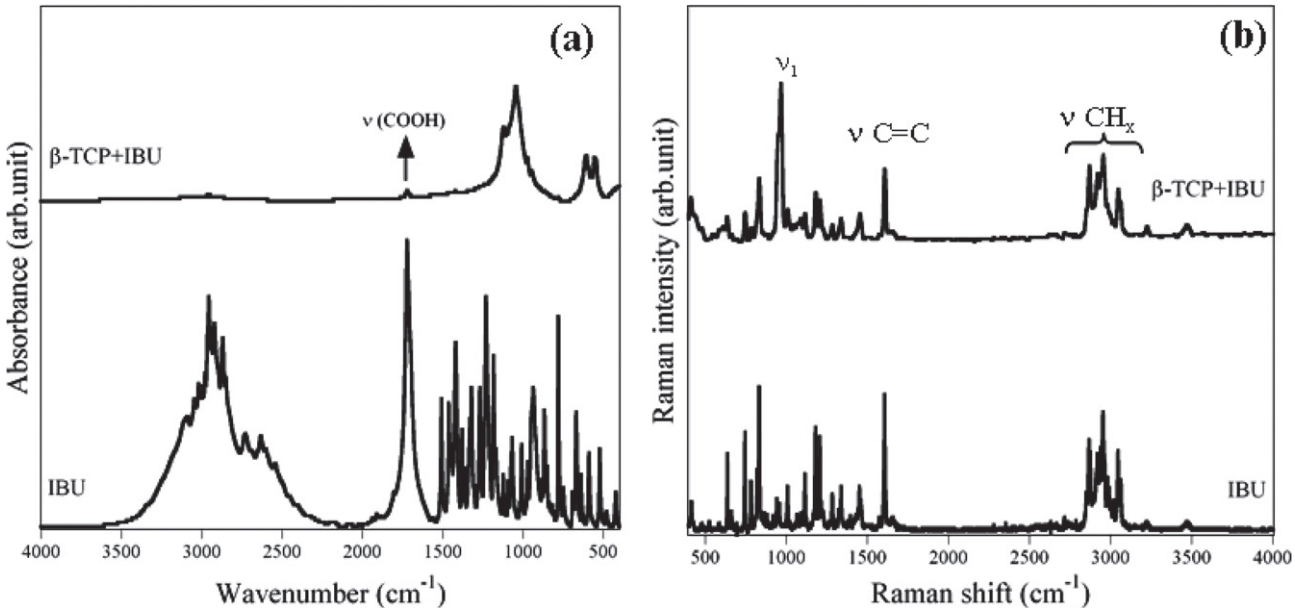

Figure 9. (a) FTIR and (b) Raman spectra of ibuprofen (IBU) and β-TCP pellets loaded with ibuprofen (β-TCP + IBU).

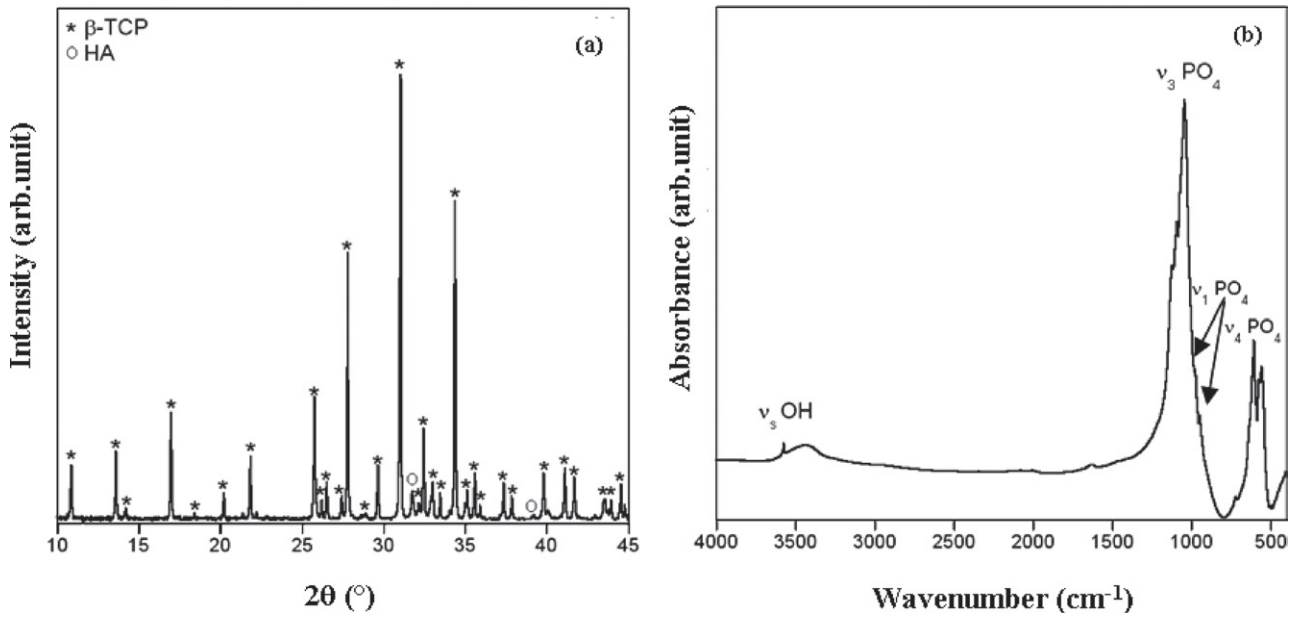

Figure 10. (a) XRD pattern and (b) FTIR spectra of β-TCP pellets after ibuprofen desorption in ethanol.

Furthermore, the XRD patterns of the loaded pellets suggest a lack of structural transformation either in the β-TCP pellets or in ibuprofen during the drug uptake. This can be related to the fact that crystallization can occur for a channel pore size significantly larger than the molecular size, about 20 times the size of the molecules [40]. Thus, the pore size of the β-TCP pellets is sufficiently large to permit the recrystallization of ibuprofen molecules (0.6–1 nm size) during the solvent evaporation. XRD, FTIR and Raman results indicate that neither adsorbed ibuprofen nor β-TCP undergo any chemical or structural modifications. These results agree with the drug adsorption behaviour.

The adsorption mechanism deduced here (i.e. physisorption) is compatible with the complete ibuprofen

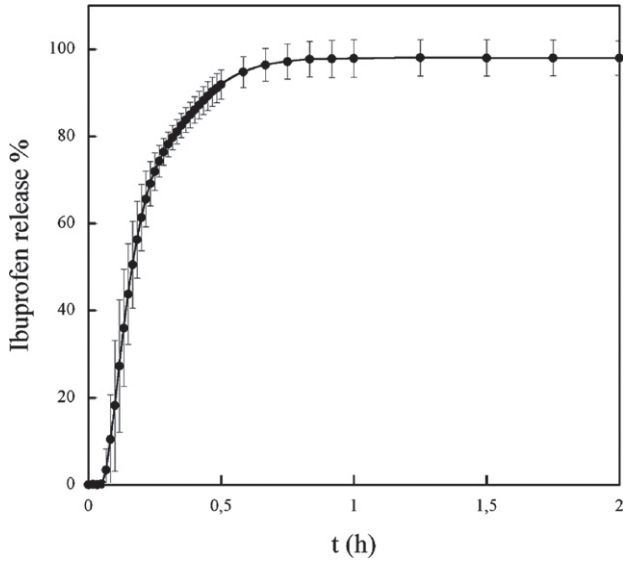

Figure 11. Ibuprofen release profile from the β-TCP pellets in phosphate buffered solution (pH = 7.5).

Table 3. Modelled drug dissolution characteristics.

Drug dissolution phase		1	2
Time (h)		0–0.25	0.25–0.46
Higuchi	R^2	0.9904	0.9955
Hixson–Crowell	R^2	0.9947	0.9994

release and it can be explained by the weak drug/substrate affinity and the coincidence of the ibuprofen adsorption and desorption isotherms.

Under the experimental conditions used for the *in vitro* dissolution trials, ibuprofen release occurred within one hour, which is considered very fast. However, note that this test was not performed to simulate *in vivo* conditions. In particular, the circulation rate of physiological fluids is weaker than the flow rate used in this work. The objectives of our experiment were to (1) verify that all ibuprofen is released into the dissolution medium, without any irreversibly adsorbed drug remaining in the pellets and (2) determine the drug dissolution mechanisms. The results show that the ibuprofen release is governed by drug erosion from the external and internal surfaces of the pellets.

In summary, the drug adsorption *via* physical interactions results in reversible drug/carrier binding without any modification of the physicochemical properties of either the drug or carrier. This property is favourable for maintaining therapeutic effects of the drug and osteoconductive properties of the carrier after the drug release. Therefore, ibuprofen-loaded β-TCP pellets are good candidates for bone defect filling and local ibuprofen delivery.

5. Conclusions

The adsorption of ibuprofen onto β-TCP porous pellets was investigated to develop an antiinflammatory delivery system for orthopaedic applications. More specifically, we aimed to reveal the type of interaction between the drug molecule and the calcium phosphate ceramic. The ibuprofen uptake by β-TCP porous pellets is very rapid, with the adsorption equilibrium attained within one hour, and the ibuprofen adsorption isotherms are described using the Freundlich equation, indicating a weak affinity between the adsorbent and adsorbate. This weak affinity was confirmed by spectroscopic measurements, which suggest that ibuprofen was adsorbed onto the β-TCP porous pellets through physisorption. No new bonds were formed during the adsorption. Thus, the ibuprofen molecule adsorbed onto the β-TCP pellets without chemical and structural modifications and its therapeutic properties should be preserved. An *in vitro* dissolution test showed the complete release of ibuprofen, and characterization of *in vivo* release kinetics and drug efficiency of the ibuprofen/β-TCP system is being planned.

Acknowledgments

The authors are grateful to the *Région Limousin* for financial support and to Nathalie Pecout for the *invitro* drug release experiments.

References

[1] LeGeros R Z 2002 *Clin. Orthop. Relat. Res* **395** 81
[2] Habraken W J E M, Wolke J G C and Jansen J A 2007 *Adv. Drug Deliv Rev.* **59** 234
[3] Vallet-Regi M 2006 *Dalton Trans.* **44** 5211
[4] Shinto Y, Uchida A, Korkusuz F, Araki N and Ono K 1992 *J. Bone Joint Surg.* B **74** 600
[5] Roussière H *et al* 2008 *Chem. Mater.* **20** 182
[6] Guicheux J, Gauthier O, Aguado E, Heymann D, Pilet P, Couillaud S, Faivre A and Daculsi G 1998 *J. Biomed. Mater. Res.* **40** 560
[7] Dion A, Berno B, Hall G and Filiaggi M J 2005 *Biomaterials* **26** 4486
[8] Victor S P and Kumar T S S 2008 *J. Biomed. Nanotechnol.* **4** 203
[9] re F, Mahmood T A, De Groot and Van Blitterswijk C A 2008 *Mater. Sci. Eng.* R **59** 38
[10] Dohzono S, Imai Y, Nakamura H, Wakitani S and Takaoka K 2009 *Clin. Orthop. Relat. Res.* **467** 3206
[11] Nandi S K, Kundu B, Ghosh S K, Mandal T K, Datta S, De D K and Basu D 2009 *Ceram. Int.* **35** 1367
[12] Romain J, Cabanas M V, Pena J, Doadrio J C and Vallet-Regi M 2008 *J. Biomed. Mater. Res.* A **84** 99
[13] Silverman L D, Lukashova L, Herman O T, Lane J M and Boskey A L 2007 *J. Orthop. Res.* **25** 23
[14] Kundu B, Lemos A, Soundrapandian C, Sen P S, Datta S, Ferreira J M F and Basu D 2010 *J. Mater. Sci.: Mater. Med.* **21** 2955
[15] Josse S *et al* 2005 *Key Eng. Mater.* **284–286** 399
[16] Doadrio A L, Sousa E M B, Doadrio J C, Pérez Pariente, Izquierdo-Barba I and Vallet-Regi M 2004 *J. Control. Release* **97** 125
[17] Vallet-Regi M, Ràmila A, Del Real R P and Pérez-Pariente J 2011 *Chem. Mater.* **13** 308
[18] Chevalier E, Viana M, Artaud A, Chomette L, Haddouchi S, Devidts G and Chulia D 2009 *AAPS PharmSciTech* **10** 597
[19] Chevalier E, Viana M, Artaud A, Haddouchi S and Chulia D 2009 *Talanta* **77** 1545
[20] Chevalier E, Viana M, Cazalbou S and Chulia D 2008 *J. Drug Deliv. Sci. Technol.* **18** 438
[21] Chevalier E, Viana M, Cazalbou S and Chulia D 2008 *Drug Dev. Ind. Pharm.* **35** 1255

[22] Chevalier E, Viana M, Cazalbou S, Makein L, Dubois J and Chulia D 2010 *Acta Biomater.* **6** 266
[23] Chevalier E, Viana M, Pouget C, Cazalbou S, Champion E and Chulia D 2009 *Bioceramics: Properties, Preparation and Applications in Follicular Lymphoma and Other Cancer Research* ed M P Safford and J G Haines (New York: Nova Sciences)
[24] Gracin S and Rasmuson A C 2002 *J. Chem. Eng. Data* **47** 1379
[25] Viana M, Jouannin P, Pontier C and Chulia D 2002 *Talanta* **57** 583
[26] Emmett P H and Brunauer S 1937 *J. Am. Chem. Soc.* **59** 1553
[27] *European Pharmacopoeia*, 7th ed. Strasbourg: Council of Europe; 2011
[28] Higuchi T 1963 *J. Pharmac. Sci.* **52** 1145
[29] Hixson AW and Crowell J H 1931 *Ind. Eng. Chem.* **23** 923
[30] AFNOR 2008 Implants chirurgicaux—Hydroxyapatite Partie 3: Analyse chimique et caractérisation de la cristallinité et de la pureté de phase, 2008
[31] Elliot J C 1994 *Structure and Chemistry of the Apatites and Other Calcium Orthophosphates* (Amsterdam: Elsevier)
[32] Cusco R, Guitia N F, De Aza A and Artus L 1998 *J. Eur. Ceram. Soc.* **18** 1301
[33] Kim J H, Kim S H, Kim H K, Akaike T and Kim S C 2002 *J. Biomed. Mater. Res.* **62** 600
[34] Benaziz L, Barroug A, Legrouri A, Rey C and Lebugle A 2001 *J. Colloid Interface Sci.* **238** 48
[35] Gbureck U, Vorndran E and Barralet J E 2008 *Acta Biomater.* **4** 1480
[36] Higgins J D, Gilmor T P, Martellucci S A, Bruce R D and Brittain H G 2001 *Anal. Profiles Drug Subst. Excipients* **27** 265
[37] Vueba M L, Pina M E and Batista De Carvalho L A E 2008 *J. Pharm. Sci.* **97** 845
[38] Charnay C, Bégu S, Tourné-Péteilh C, Nicole L, Lerner D A and Devoisselle J M 2004 *Euro. J. Pharm. Biopharm.* **57** 533
[39] Stähli C, Bohner M, Bashoor-Zadeh M, Doebelin N and Baroud G *Acta Biomater.* **6** 2760
[40] Sliwinska-Bartkowiak M, Dudziak G, Gras R, Sikorski R, Radhakrishnan R and Gubbins K E 2001 *Colloids Surf.* A **187–188** 523